AGU100 ADVANCING EARTH AND SPACE SCIENCE

JGR Biogeosciences

RESEARCH ARTICLE
10.1029/2019JG005402

Exploring the Temperature Dependence of Clumped Isotopes in Modern *Porites* Corals

Yangrui Guo[1,2,3], Wenfeng Deng[1,3,4], Gangjian Wei[1,3], Xuefei Chen[1,3], Xi Liu[1], Xijie Wang[1,2], Li Lo[1,5], Guanqiang Cai[6], and Ti Zeng[1,3]

[1]State Key Laboratory of Isotope Geochemistry, Guangzhou Institute of Geochemistry, Chinese Academy of Sciences, Guangzhou, China, [2]College of Earth and Planetary Sciences, University of Chinese Academy of Sciences, Beijing, China, [3]Southern Marine Science and Engineering Guangdong Laboratory, Guangzhou, China, [4]Radiogenic Isotope Facility, School of Earth and Environmental Sciences, The University of Queensland, Brisbane, Queensland, Australia, [5]Now at Department of Geosciences, National Taiwan University, Taipei, Taiwan, [6]Guangzhou Marine Geological Survey, China Geological Survey, Guangzhou, China

Key Points:
- There is no evidence of intercolony or intracolony variations in mean Δ_{47} values of *Porites* corals on an annual timescale
- Coral vital effects are found to cause relative disequilibrium of isotopic composition at an intracolony level
- Clumped isotopes analysis of *Porites* corals is suitable for reconstructing relative changes in seasonal sea surface temperature

Correspondence to:
W. Deng,
wfdeng@gig.ac.cn;
w.deng@uq.edu.au

Citation:
Guo, Y., Deng, W., Wei, G., Chen, X., Liu, X., Wang, X., et al. (2020). Exploring the temperature dependence of clumped isotopes in modern Porites corals. *Journal of Geophysical Research: Biogeosciences*, *125*, e2019JG005402. https://doi.org/10.1029/2019JG005402

Received 28 JUL 2019
Accepted 6 NOV 2019
Accepted article online 28 NOV 2019

Abstract *Porites* corals are valuable geological archives for reconstructing past sea surface temperature (SST) in tropical oceans. Their clumped isotope compositions (indicated by Δ_{47} values) provide a potential proxy for SST. The Δ_{47} value in *Porites* coral usually departs from thermodynamic equilibrium due to vital effects. To explore the temperature dependence of Δ_{47} values in corals, we determined $\delta^{13}C$, $\delta^{18}O$, and Δ_{47} values in two modern *Porites* corals from the South China Sea. Our results indicate no intercolony or intracolony biases in Δ_{47} values on annual timescales. However, on seasonal timescales, Δ_{47} enrichment associated with $\delta^{13}C$ depletion is observed at an intracolony level. This cannot be explained by incomplete hydration and/or hydroxylation of metabolic CO_2; instead, we interpret this new pattern of isotopic anomalies as a peculiar evidence of vital effects on Δ_{47} and $\delta^{13}C$ fractionation. Although complicated by vital effects, the Δ_{47} signature in *Porites* corals still preserved a robust SST dependence, similar to those of recently published Δ_{47}-T calibrations. The observed Δ_{47} offset relative to inorganic carbonate due to the vital effects is consistent, and relative variations in seasonal SST can be obtained. This study refines the Δ_{47} thermometer in *Porites* corals and strengthens its capacity to be used to reconstruct past SST.

Plain Language Summary Sea surface temperature (SST) is a fundamental parameter of climate variation. Understanding how SST has changed in the past is important to inform climate predictions. One way to do this is by developing a reliable thermometer based on the clumped isotope composition (Δ_{47}) of corals. However, the thermometer based on coral Δ_{47} values may be complicated by biological factors that affect the Δ_{47} values as the coral grows. We investigated two modern *Porites* corals from the South China Sea by measuring their oxygen, carbon, and clumped isotope compositions. By comparing two samples from the same coral colony, we found that the impact of biological factors is significant, causing unusual patterns in the carbon and clumped isotopes. The biological factors also likely lead to differences in the coral Δ_{47} values from two different colonies. To account for these potential intracolony and intercolony effects, we established a relationship between the Δ_{47} values and SST based on the two corals. This relationship has the same temperature dependence as other Δ_{47} thermometers established on synthetic carbonates in which no biological factors are involved and can be used as a thermometer to reconstruct seasonal SST.

1. Introduction

The $\delta^{18}O$ values and Sr/Ca ratios of *Porites* coral skeletons have been widely used to reconstruct past sea surface temperature (SST; Beck et al., 1992; Felis et al., 2000; Gagan et al., 1998; McCulloch et al., 1999; Smith et al., 1979). However, the applications of these two proxies can be problematic. The use of coral $\delta^{18}O$ to reconstruct SST requires knowledge of the past seawater $\delta^{18}O$ values, which are difficult to constrain (Shackleton, 1967). It can be further complicated by isotopic disequilibrium fractionation as the coral skeletons are commonly depleted in ^{18}O compared to inorganic aragonites under identical precipitation conditions. This is caused by "vital effects," a term that encompasses the various biological factors that take place during coral skeleton calcification (Weber & Woodhead, 1972). This $\delta^{18}O$ disequilibrium (up to several ‰) can override most of temperature signals in the coral $\delta^{18}O$. Similarly, coral Sr/Ca ratios show disequilibrium with respect to inorganic aragonite and can be affected by seawater Sr/Ca variations (de Villiers

et al., 1995). These disequilibrium offsets in $\delta^{18}O$ values and Sr/Ca ratios are usually assumed to be correctable by sampling the maximum growth axis of corals (Linsley et al., 1999) or analyzing samples with appropriate skeletal extension rates (Felis et al., 2003; Mitsuguchi et al., 2003). However, factors controlling the disequilibrium of both $\delta^{18}O$ values and Sr/Ca ratios in corals remain elusive.

The clumped isotope composition of carbonates offers an opportunity to extract a seawater temperature signal from coral skeletons without needing to know the composition of the water where the coral grew (Ghosh et al., 2006). This novel method of thermometry is based on the temperature dependence of the ^{13}C–^{18}O bond ordering within carbonate lattices, with Δ_{47} value being defined as

$$\Delta_{47} = \left[\left(\frac{R^{47}}{R^{47*}}-1\right)-\left(\frac{R^{46}}{R^{46*}}-1\right)-\left(\frac{R^{45}}{R^{45*}}-1\right)\right]\times 1,000‰ \quad (1)$$

where R is the measured ratio of isotopologues of molecular mass 47, 46, or 45 relative to mass 44 and R^* indicates calculated stochastic ratios where all isotopes are randomly distributed among the isotopologues (Eiler, 2007; Huntington et al., 2009). At higher temperatures, ^{13}C and ^{18}O tend to distribute randomly among all isotopologues during chemical bonding, leading to low Δ_{47} values. At lower temperatures, ^{13}C and ^{18}O tend to clump together within the same carbonate ion groups, resulting in high Δ_{47} values (Wang et al., 2004).

The Δ_{47} values of modern corals have been analyzed to assess their capacity for constraining seawater temperatures (Ghosh et al., 2006; Kimball et al., 2016; Saenger et al., 2012; Saenger et al., 2017; Spooner et al., 2016; Thiagarajan et al., 2011). Significant positive deviations in Δ_{47} values relative to those of inorganic carbonates at the same temperature have been observed in some *Porites* corals (Ghosh et al., 2006; Saenger et al., 2012). Saenger et al. (2012) compared kinetic differences in dissolved inorganic carbon (DIC) species between biogenic coral and inorganic carbonate precipitation environments, suggesting that Δ_{47} disequilibria are likely associated with the low kinetics of the hydration/hydroxylation of metabolic CO_2, which is induced from vital effects during coral calcification. They attempted to elucidate the influence of biological factors by examining Δ_{47} differences among samples with variable extension rates at an intracolony level on annual timescales. However, the extent to which Δ_{47} differences can be explained by the kinetic isotopic effects of hydration/hydroxylation of CO_2 on seasonal timescales remains open to question. The Δ_{47} signature along an "isochron" within the one single colony on a seasonal timescale is potentially a good test for a vital effect model because the environmental conditions will be consistent in the isochronal skeletons and the test is independent of isotopic differences between coral and inorganic carbonates. Nevertheless, vital effects likely compromise the application of the coral Δ_{47} thermometer on seasonal timescales and a more thorough exploration of the seasonal temperature dependence of Δ_{47} values in corals is needed.

Here, we explore the signatures of clumped isotope composition in two modern *Porites* corals from inshore and offshore coral reefs in the South China Sea with well-constrained environmental records. We focus on examining the vital effects through comparing the relative differences of isotopic compositions within the isochronal skeletons in one colony where environmental conditions are assumed to be consistent. This study both advances new evidence of vital effects acting upon the clumped isotope composition of *Porites* corals on seasonal timescales and strengthens the capacity of the Δ_{47} value of the coral for reconstructing relative variations in seasonal SST.

2. Materials and Methods

2.1. Coral Sampling and Pretreatment

Two specimens of living *Porites* colonies were collected from Sanya Bay and Qilianyu Islet in the northern South China Sea (Figure 1a). The coral colony 16SYS was collected in April 2016 from a water depth of ~3 m on a fringe reef in Sanya Bay (18.218°N; 109.484°E), on the southernmost of Hainan Island (Figure 1b). The coral core 15XS was drilled using underwater drilling techniques from a living coral colony in September 2015, from a water depth of ~2.5 m at Qilianyu Islet (16.948°N; 112.333°E). The islet is located in an arced reef flat consisting of several small lagoon islands within the Xisha Islands (Figure 1c).

Coral samples were cut into ~8 mm thick slabs using a rock-cutting saw, parallel to the growth axis identified in X-ray images (Figure 2). The slabs were soaked in 10% H_2O_2 for 24 hr at room temperature to remove

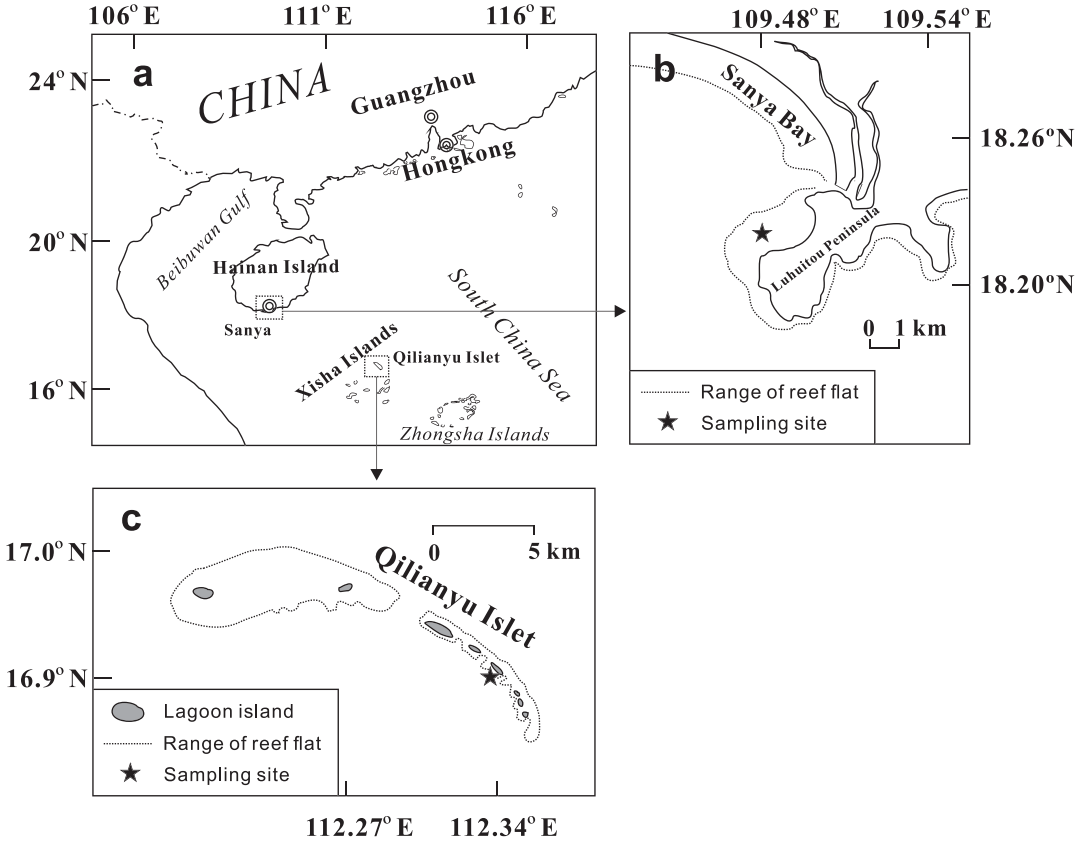

Figure 1. Map showing locations of sampling sites.

organic matter, cleaned ultrasonically with deionized water, and dried at 50 °C. This oxidative cleaning method does not affect the carbonate Δ_{47} values (Guo et al., 2019; Saenger et al., 2012). The Sanya Bay coral was sampled along two sampling tracks (16SYST1 and 16SYST2), and the Qilianyu Islet coral was sampled along a single track (15XS15; Figure 2). The tracks were sampled at 1 mm intervals using a low-speed carving drill (JSDA®) equipped with a 0.8 mm diameter bit. The slow drill speed was chosen to minimize drill heating, which likely affects isotopic compositions and induces mineral transition (Staudigel & Swart, 2016). The excavated regions were 5 mm wide and 5 mm deep and yielded ~30 mg of sample powder. To avoid cross contamination, the residual powders on the slab and drill bit were carefully removed between samples. Samples were homogenized using an agate mortar and pestle in preparation for Sr/Ca ratio and isotope analyses.

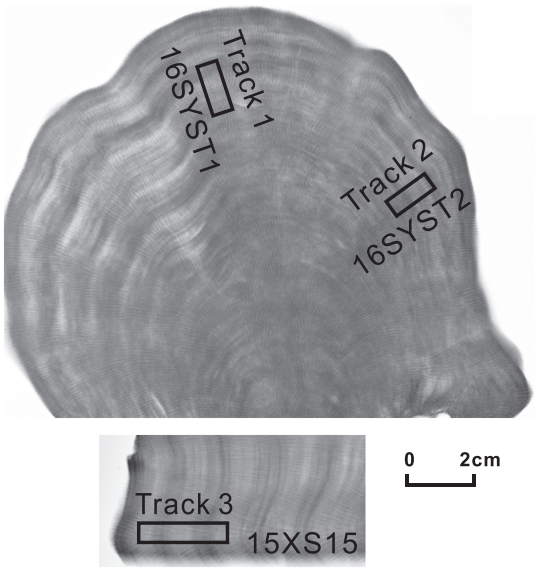

Figure 2. Positive X-ray images showing three sampling tracks. The black frames indicate the sampling tracks for Sr/Ca and isotopic analyses.

2.2. Sr/Ca and Isotopic Analyses

The Sr/Ca ratios of the samples were determined using a Varian Vista Pro inductively coupled plasma atomic emission spectrometer based on the method described by Wei et al. (2007). Each sample of ~2 mg was weighted and dissolved in 2% HNO_3 at room temperature. The solution was diluted to 10,000 times prior to the Sr/Ca measurement. An in-house standard solution, BH-7, with a Sr/Ca ratio normalized against the JCp-1 standard (Wang et al., 2018) was repeatedly measured every five samples to correct for short-term instrumental drift. Its external precision of Sr/Ca analyses was ~0.02 mmol mol^{-1} based on repeated measurements of the BH-7 standard.

Isotopic composition measurements ($\delta^{13}C$, $\delta^{18}O$, and Δ_{47}) were conducted at the State Key Laboratory of Isotope Geochemistry, Guangzhou Institute of Geochemistry, Chinese Academy of Sciences, Guangzhou, China, using an isotope ratio mass spectrometer (IRMS; Thermo Scientific^{TM} 253 Plus) coupled to a dual-inlet system. Samples of at least one full year of growth identified from annual Sr/Ca cycles were selected for isotopic analyses of which the sampling tracks were indicated by black frames (Figure 2). Note that the outer part of the skeletons was avoided due to possible contamination from coral tissues. Each powder sample was analyzed with at least three replicates. For each replicated analysis, carbonate acid digestion, gas purification, and data treatment followed the methods described by Guo et al. (2019). Specifically, 4–7 mg of carbonate samples or standards were digested with orthophosphoric acid (1.92–1.96 g mL^{-1}) at 90 °C for ~15 min. The released CO_2 was collected in a liquid nitrogen trap on a vacuum line as described by Guo et al. (2019). The trap was subsequently warmed by ethanol slush (−90 °C) to remove water, and the released CO_2 was passed through an absorbent trap (PoraPak^{TM} Q at −20 °C) to remove contaminants. The gas was then cleaned by another ethanol slush trap (−90 °C) and finally collected in a glass tube before being introduced to the IRMS. Yields of CO_2 were estimated using the inlet pressure gauge on the IRMS, with no gas loss being observed for pure calcium carbonate samples.

The instrument was configured to measure the intensity of signals at masses 44, 45, and 46 (amplified by 3×10^8, 3×10^{10}, and 1×10^{11} Ω resistors, respectively) and 47, 48, and 49 (all amplified by 1×10^{13} Ω resistors) with a half cup (collecting signals of mass 47.5) for monitoring the internal background. The measuring intensity of mass 44 was adjusted to 10 V on both sample and reference sides. Each analysis involved six measurements with a total of 60 cycles with 26 s integration time and 12 s changeover delay per cycle. Peak centering was automatically performed before each measurement. Internal precision of each analysis was normally around 0.009‰ (1 standard error), close to the theoretical counting limit (Merritt & Hayes, 1994). Raw data files from the IRMS were processed with Easotope software (John & Bowen, 2016) to obtain raw Δ_{47} values and bulk $\delta^{13}C$ and $\delta^{18}O$ values. The ^{17}O correction method of Brand et al. (2010) was used during the data calculation as previous studies (Daëron et al., 2016; Schauer et al., 2016). The acid digestion fractionation factor for oxygen isotopes in aragonite of Kim, Mucci, et al. (2007) was applied. To normalize Δ_{47} values to a reference frame at a digestion temperature of 25 °C, an acid digestion fractionation factor (AFF) of 0.068‰ was used as experimentally determined by Guo et al. (2019) within the same laboratory in this study. This AFF is close to the value of 0.069‰ predicted based on theoretical calculation by Guo, Mosenfelder, et al. (2009) and also similar to the value of 0.066‰ experimentally determined for aragonite by Wacker et al. (2013).

The $\delta^{13}C$ and $\delta^{18}O$ values are reported relative to Vienna Pee Dee Belemnite (VPDB) using a high-purity CO_2 reference gas normalized to the NBS-19 standard. CO_2 gases equilibrated at 1,000 °C (heated gases) were prepared as described by Huntington et al. (2009). These heated gases vary in bulk $\delta^{13}C$ and $\delta^{18}O$ values but have the same Δ_{47} value due to the stochastic distribution achieved at high temperatures. They were analyzed regularly to correct for the instrument nonlinearity, as suggested by Huntington et al. (2009). Two carbonate standards, C1 and BACS, were analyzed almost daily to monitor instrumental drift. Their Δ_{47} values at an absolute reference frame (ARF) scale were determined by Guo et al. (2019) by using the heated gases and CO_2 gas equilibrated at 25 °C as suggested by Dennis et al. (2011). To monitor and correct the scale compression during different analytical periods, standards C1 and BACS were used to establish a measured versus accepted Δ_{47} value relationship as the secondary transfer function described by Dennis et al. (2011). The raw Δ_{47} value of a sample carbonate was first corrected for nonlinearity effects using heated gas data and then reported at the ARF scale through the secondary transfer function. Measurement contamination was evaluated by Δ_{48} values based on the method of Huntington et al. (2009). If the Δ_{48} values of the sample or standard gas are more than 1‰ higher than those of heated gases with similar δ_{48} values, the data were discarded.

The long-term precisions of carbonate standards are ~0.015‰ for Δ_{47}, ~0.02‰ for $\delta^{13}C$, and ~0.08‰ for $\delta^{18}O$ (1σ, with ~30 replicates for each standard). Two international clumped isotope standards, ETH2 and ETH4, were also analyzed. Their mean values during the measuring periods are 0.305 ± 0.018‰ (1σ, $n = 13$) and 0.531 ± 0.015‰ (1σ, $n = 16$), respectively, similar to those reported previously (Daëron et al., 2016; Schauer et al., 2016). All the raw isotopic data of the samples and standards are available on Zenodo (Guo, 2019).

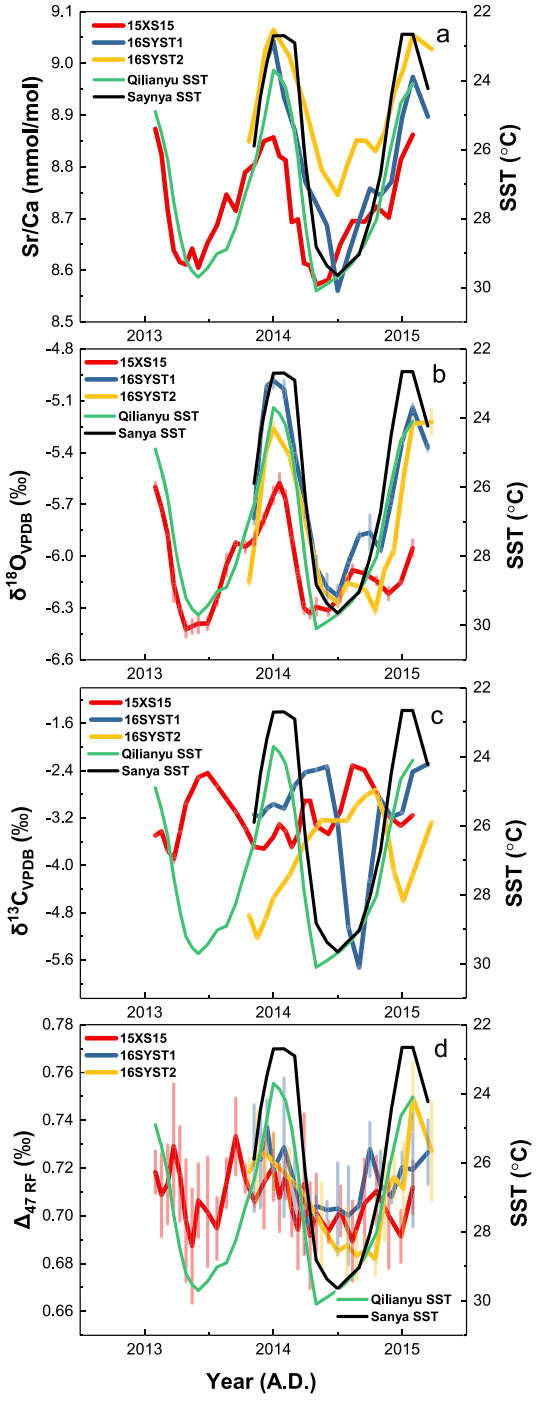

Figure 3. Time series of Sr/Ca ratios and isotopic compositions for the three coral sampling tracks. (a) Sr/Ca; (b) $\delta^{18}O$; (c) $\delta^{13}C$; (d) $\Delta_{47\ RF}$. Δ_{47} values are reported at ARF scale and corrected with AFF of 0.068‰. Error bars represent 2σ associated with the analytical precision. The green and black lines represent the SST records of Sanya Bay and Qilianyu Islet, respectively.

2.3. SST Records and Time Series Treatment

To estimate the calcification temperatures of the coral skeletons, monthly HadISST data covering the study sites were used (1° × 1°, http://coastwatch.pfeg.noaa.gov/erddap/griddap/erdHadISST.html) with an assumption that the waters at a few meters depth are well mixed with the surface. These long-term SST records show clear seasonal variations, with maximum and minimum SST generally occurring in June and January each year, respectively.

Sr/Ca ratios were used to adjust isotopic data to a common time frame as all Sr/Ca and isotopic data were measured on the same sample aliquots. Sr/Ca maxima and minima were tied to the SST minima and maxima in each annual cycle. As all tracks were analyzed at >12 samples per year, the monthly SST records were linearly interpolated to assign the calcification temperature for each sample by using PAST3 software (Hammer et al., 2001). To explore isotopic difference at an intracolony level, we need to compare the relative differences in isotopic compositions between isochronal skeletons (in the case of Track 1 versus Track 2). However, the data points from the two tracks did not exactly match each other on the same timescale. We therefore set a decimal time period of 2013.8 to 2015.1, which is concurrently covered by both the tracks. To keep a similar time resolution as that revealed by the data points, the periods were divided into 13 intervals with each interval representing a decimal time length of 0.1. The isotopic composition of each interval was obtained by averaging or binning the isotopic data of the samples within the interval.

3. Results

All Sr/Ca and $\delta^{18}O$ time series from two coral colonies showed similar seasonal patterns that coincided with SST (Figures 3a and 3b). Sr/Ca ratios in Qilianyu Islet coral ranged between 8.58 and 8.86 mmol mol^{-1}, and the Sanya Bay coral ranged from 8.56 to 9.06 mmol mol^{-1} (Table 1). Coral $\delta^{18}O$ values ranged from −6.4‰ to −5.6‰ in the Qilianyu Islet coral and −6.3‰ to −5.0‰ for the Sanya Bay coral (Table 1). Coral $\delta^{13}C$ values did not show any regular seasonal patterns, and there were significant differences between the three time series (Figure 3c). The Sanya Bay and Qilianyu Islet corals had $\delta^{13}C$ variation ranges of ~3.3‰ and ~1.6‰, respectively. The $\delta^{13}C$ maxima occurred in late summer of 2014 in tracks 15XS15 and 16SYST2, but in 16SYST1 they were lower at that time. Coral Δ_{47} values showed no significant seasonal pattern. However, lower Δ_{47} values generally occurred in summer and higher values in winter (Figure 3d). The Δ_{47} values were in the ranges 0.687‰–0.733‰ in track 15XS15, 0.697‰–0.737‰ in 16SYST1, and 0.683‰–0.750‰ in 16SYST2. Note that the two locations exhibit small difference (~1 °C) in winter SST. Such difference cannot be resolved by the Δ_{47} values. As considering the analytical uncertainty of ~0.015‰, the ranges of Δ_{47} values from the three sampling tracks broadly overlapped with each other (Figure 3d).

4. Discussion

4.1. Clumped Isotope Vital Effects at an Intracolony Level

The differences between the coral calcifying fluid and an inorganic carbonate solution can provide possible clues in elucidating vital effects manifested by the positive offsets in coral Δ_{47} values relative to inorganic

Table 1
Geochemical Data in Coral Skeleton Carbonate

Sample ID	Temp. (°C)	Date	Sr/Ca (mmol mol^{-1})	$\delta^{13}C_{VPDB}$ (‰)	1σ	$\delta^{18}O_{VPDB}$ (‰)	1σ	$\Delta_{47\ RF}$ (‰)	1σ	n
15XS15-10	24.1	2015.08	8.86	−3.15	0.01	−5.95	0.05	0.712	0.011	3
15XS15-11	24.7	2014.99	8.81	−3.33	0.01	−6.15	0.01	0.691	0.011	3
15XS15-12	26.2	2014.90	8.70	−3.17	0.01	−6.22	0.04	0.700	0.022	3
15XS15-13	28.0	2014.80	8.72	−2.77	0.01	−6.14	0.02	0.710	0.015	3
15XS15-14	28.8	2014.71	8.69	−2.39	0.00	−6.10	0.03	0.705	0.019	3
15XS15-15	29.3	2014.61	8.70	−2.31	0.01	−6.08	0.03	0.689	0.017	3
15XS15-16	29.6	2014.52	8.65	−3.09	0.00	−6.23	0.04	0.702	0.010	3
15XS15-17	29.9	2014.43	8.58	−3.47	0.00	−6.31	0.03	0.693	0.005	3
15XS15-18	30.1	2014.33	8.57	−3.34	0.01	−6.29	0.05	0.701	0.016	3
15XS15-19	29.1	2014.29	8.61	−2.91	0.00	−6.33	0.03	0.692	0.022	3
15XS15-20	27.9	2014.24	8.61	−2.91	0.00	−6.30	0.03	0.713	0.029	4
15XS15-21	26.2	2014.19	8.70	−3.49	0.01	−6.10	0.03	0.694	0.016	3
15XS15-22	25.0	2014.14	8.69	−3.69	0.02	−5.89	0.04	0.703	0.011	3
15XS15-23	24.2	2014.10	8.81	−3.42	0.01	−5.67	0.05	0.717	0.010	3
15XS15-24	23.9	2014.05	8.82	−3.31	0.02	−5.58	0.06	0.708	0.014	3
15XS15-25	23.7	2014.00	8.86	−3.52	0.00	−5.65	0.05	0.721	0.014	3
15XS15-26	25.2	2013.93	8.85	−3.72	0.00	−5.79	0.04	0.714	0.019	3
15XS15-27	26.5	2013.85	8.80	−3.69	0.01	−5.90	0.04	0.706	0.002	3
15XS15-28	27.3	2013.78	8.79	−3.37	0.02	−5.95	0.03	0.716	0.006	3
15XS15-29	28.3	2013.71	8.71	−3.10	0.01	−5.92	0.01	0.733	0.016	4
15XS15-30	28.9	2013.64	8.75	−2.88	0.00	−6.05	0.06	0.714	0.010	3
15XS15-31	29.0	2013.56	8.69	−2.66	0.01	−6.24	0.04	0.695	0.013	3
15XS15-32	29.4	2013.49	8.65	−2.44	0.00	−6.39	0.03	0.702	0.023	3
15XS15-33	29.7	2013.42	8.60	−2.51	0.01	−6.39	0.05	0.706	0.015	3
15XS15-34	29.5	2013.37	8.64	−2.74	0.00	−6.41	0.04	0.687	0.024	3
15XS15-35	29.2	2013.32	8.61	−2.95	0.01	−6.42	0.05	0.698	0.025	3
15XS15-36	28.5	2013.27	8.62	−3.44	0.01	−6.31	0.03	0.718	0.020	4
15XS15-37	27.5	2013.23	8.64	−3.89	0.07	−6.17	0.10	0.729	0.026	4
15XS15-38	26.3	2013.18	8.72	−3.74	0.01	−5.87	0.03	0.713	0.017	3
15XS15-39	25.5	2013.13	8.82	−3.43	0.01	−5.72	0.03	0.709	0.018	3
15XS15-40	24.9	2013.08	8.87	−3.50	0.01	−5.60	0.03	0.718	0.009	3
16SYST1-22	24.2	2015.20	8.90	−2.29	0.00	−5.37	0.02	0.727	0.013	3
16SYST1-23	22.7	2015.08	8.97	−2.42	0.00	−5.14	0.02	0.719	0.024	3
16SYST1-24	22.7	2015.00	8.89	−3.11	0.01	−5.34	0.01	0.720	0.007	3
16SYST1-25	24.5	2014.92	8.77	−3.18	0.01	−5.67	0.03	0.708	0.003	3
16SYST1-26	26.7	2014.83	8.74	−2.89	0.01	−5.97	0.01	0.713	0.014	3
16SYST1-27	28.1	2014.75	8.76	−4.24	0.02	−5.86	0.10	0.728	0.011	3
16SYST1-28	29.0	2014.67	8.70	−5.73	0.01	−5.88	0.02	0.704	0.002	3
16SYST1-29	29.3	2014.58	8.63	−5.05	0.02	−6.04	0.03	0.700	0.021	3
16SYST1-30	29.7	2014.50	8.56	−3.29	0.01	−6.23	0.06	0.703	0.019	3
16SYST1-31	29.4	2014.42	8.69	−2.33	0.01	−6.18	0.08	0.702	0.004	3
16SYST1-32	28.8	2014.33	8.73	−2.39	0.01	−6.07	0.07	0.704	0.004	3
16SYST1-33	26.4	2014.25	8.77	−2.43	0.01	−5.71	0.07	0.696	0.012	3
16SYST1-34	22.9	2014.17	8.87	−2.65	0.01	−5.41	0.06	0.713	0.016	3
16SYST1-35	22.7	2014.08	8.93	−3.04	0.00	−5.03	0.05	0.729	0.029	4
16SYST1-36	22.7	2014.00	9.04	−2.97	0.01	−4.98	0.05	0.719	0.009	3
16SYST1-37	23.5	2013.95	9.01	−3.04	0.01	−5.02	0.01	0.737	0.011	4
16SYST1-38	24.5	2013.90	8.95	−3.18	0.01	−5.30	0.01	0.724	0.020	3
16SYST1-39	25.9	2013.85	8.89	−3.15	0.01	−5.78	0.04	0.724	0.022	4
16SYST2-14	24.9	2015.23	9.03	−3.28	0.02	−5.22	0.07	0.727	0.021	3
16SYST2-15	22.7	2015.08	9.06	−4.16	0.01	−5.23	0.04	0.750	0.014	3
16SYST2-16	22.7	2015.01	8.99	−4.60	0.01	−5.55	0.06	0.711	0.019	3
16SYST2-17	24.0	2014.94	8.94	−4.10	0.03	−5.96	0.04	0.716	0.009	3
16SYST2-18	25.9	2014.86	8.87	−3.16	0.00	−6.08	0.03	0.709	0.020	2
16SYST2-19	27.4	2014.79	8.83	−2.73	0.00	−6.32	0.02	0.682	0.007	2
16SYST2-20	28.4	2014.72	8.85	−2.82	0.02	−6.20	0.03	0.686	0.005	3
16SYST2-21	29.1	2014.65	8.85	−2.98	0.01	−6.17	0.01	0.683	0.010	3
16SYST2-22	29.4	2014.57	8.80	−3.24	0.02	−6.16	0.05	0.688	0.016	3
16SYST2-23	29.7	2014.50	8.75	−3.25	0.00	−6.27	0.02	0.685	0.002	3
16SYST2-24	29.1	2014.38	8.79	−3.24	0.02	−6.19	0.04	0.696	0.018	3

Table 1
(continued)

Sample ID	Temp. (°C)	Date	Sr/Ca (mmol mol^{-1})	$\delta^{13}C_{VPDB}$ (‰)	1σ	$\delta^{18}O_{VPDB}$ (‰)	1σ	$\Delta_{47\ RF}$ (‰)	1σ	n
16SYST2-25	26.4	2014.25	8.91	−3.61	0.00	−5.80	0.01	0.709	0.005	3
16SYST2-26	22.8	2014.13	9.01	−4.17	0.01	−5.42	0.01	0.716	0.012	3
16SYST2-27	22.7	2014.00	9.06	−4.55	0.01	−5.26	0.04	0.722	0.012	3
16SYST2-28	23.7	2013.94	9.03	−4.92	0.01	−5.41	0.02	0.726	0.011	3
16SYST2-29	25.2	2013.88	8.93	−5.23	0.01	−5.82	0.02	0.725	0.019	3
16SYST2-30	26.7	2013.81	8.85	−4.84	0.01	−6.15	0.02	0.718	0.006	3

Note. $\delta^{18}O$ and $\delta^{13}C$ values are reported relative to VPBD. $\Delta_{47\ RF}$ values are reported in ARF scale and corrected with AFF of 0.068‰. 1σ refers to 1 standard deviation of the mean value for multiple replicates. "Temp" refers coral calcification temperature estimated from satellite SST records.

carbonates (Ghosh et al., 2006; Saenger et al., 2012). Relative disequilibrium fractionations within a coral colony can be observed by comparing the isotopic compositions of two isochronal tracks (16SYST1 and 16SYST2) within the same coral colony. Isotopic variation between two isochronal tracks is presumed to be independent of variations in seawater temperature or isotopic composition. As the two sampled regions have experienced identical growth conditions, any variation between the two tracks' isotopic compositions would be directly related to nonenvironmental factors, providing a useful perspective in exploring the influence of vital effects on coral Δ_{47} values.

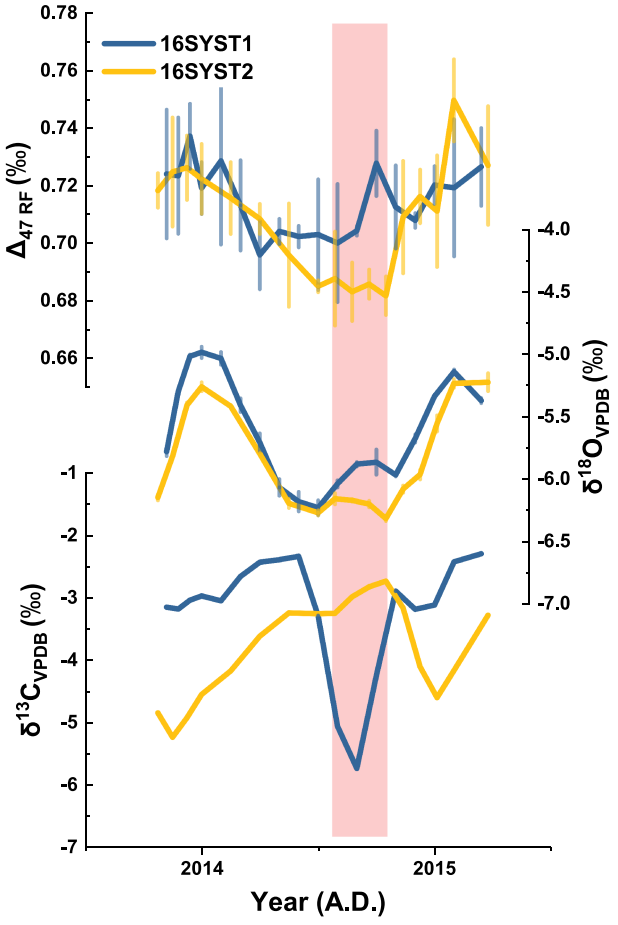

Figure 4. Intracolony differences in Δ_{47}, $\delta^{18}O$, and $\delta^{13}C$ values. The isotopic differences between two sampling tracks are indicative of vital effects during the coral growth within the one single colony. The approximate period of the late summer of 2014 is shaded in pink, indicating the highest differences in isotopic compositions between two sampling tracks. Error bars represent 2σ associated with the analytical precision.

As shown in Figure 4, the two tracks exhibit broadly similar $\delta^{18}O$ profiles with slight differences (<0.3‰) during early spring and late summer of 2014, but there are significant differences in their Δ_{47} (>0.04‰) and $\delta^{13}C$ (>2‰) values. The most significant indication of vital effects are the enrichments in Δ_{47} and corresponding depletions in $\delta^{13}C$ in track 16SYST1 relative to 16SYST2, observed during the late summer of 2014 (Figure 4). In corals, photosynthesis increases skeletal $\delta^{13}C$ values through selective removal of ^{12}C from the metabolic CO_2, which leads to enrichment of ^{13}C in the calcifying fluid; coral respiration has the opposite effect and decreases the skeletal $\delta^{13}C$ values (Goreau, 1977; Schoepf et al., 2014; Weber, 1974). As the corals of the two sampling tracks were from the same colony and likely experienced similar light intensities, we assume that photosynthesis of symbiotic zooxanthellae in the corals takes place in a similar manner within each sampling tracks. As such, the relatively high depletion in skeletal $\delta^{13}C$ in track 16SYST1 likely reflects higher amounts of metabolic CO_2 induced from a higher degree of respiration by the zooxanthellae and the host coral, rather than any effects from photosynthesis.

The relative depletion in $\delta^{13}C$ can be a proxy for excess metabolic CO_2 or the state of the metabolism of symbiotic zooxanthellae and the host coral. If the CO_2 is the main carbon source for coral calcification, this higher CO_2 concentration possibly has a greater influence upon Δ_{47} vital effects during the hydration/hydroxylation process (Saenger et al., 2012). This could explain the relative enrichment of Δ_{47}. However, the theoretical calculations of Guo, Kim, et al. (2009) indicate that enrichment of Δ_{47} via this mechanism should be accompanied synchronous depletion of $\delta^{18}O$, but the $\delta^{18}O$ profiles of two sampling tracks do not exhibit large differences (Figure 4).

To discriminate between the potential factors governing isotopic fractionation in corals observed in this study, we explored the isotopic signatures in the $\Delta(\Delta_{47})$-$\Delta(\delta^{18}O)$ and $\Delta(\Delta_{47})$-$\Delta(\delta^{13}C)$ panels (Figure 5). The Δ values

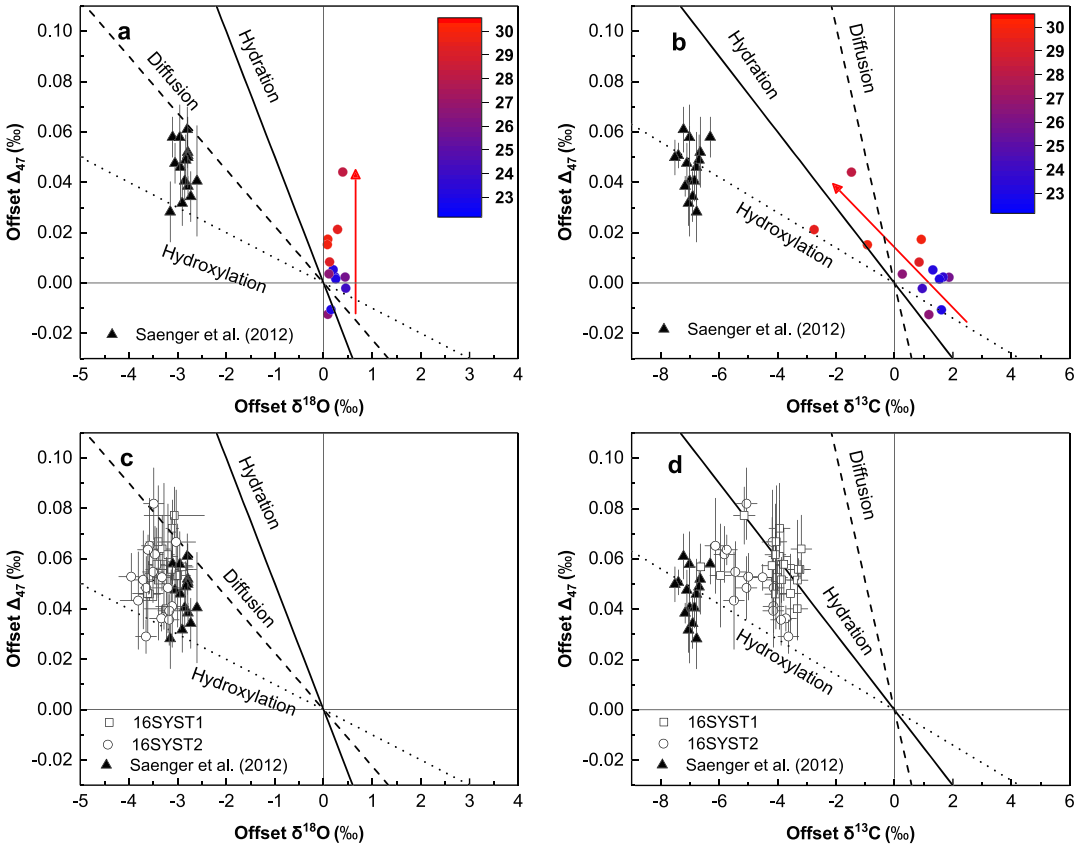

Figure 5. Comparison of isotopic offsets with theoretical predictions for the fractionation effect of CO_2 diffusion (black dashed line), hydration (black solid line), and hydroxylation (black dotted line) based on previous studies (Guo, Kim, et al., 2009; Saenger et al., 2012; Thiagarajan et al., 2011). The data of Saenger et al. (2012) in all panels are based on *Porites* corals and are defined as the offset of the measured values relative to their respective equilibrium values. The colored data points (panel a and b) are the offsets of the binned isotopic compositions of track 16SYST1 relative to 16SYST2. The color suggests different growth temperatures. The red arrows indicate the directions of disequilibrium fractionation. The data from this study in the panel c and d are defined as the offset of the measured values relative to their respective equilibrium values. The Δ_{47} at equilibrium is predicted with the Δ_{47}–T calibration of Kelson et al. (2017). The $\delta^{18}O$ at equilibrium is calculated based on the aragonite-water fractionation factor of Kim, O'Neil, et al. (2007), the SST record, and the $\delta^{18}O$ value of seawater ($\delta^{18}O_{seawater}$). The $\delta^{18}O_{seawater}$ is estimated from in situ sea surface salinity (SSS) record at Sanya Bay and a $\delta^{18}O_{seawater}$–SSS relationship ($\delta^{18}O_{seawater} = 0.23 \times SSS - 7.78$, $r^2 = 0.67$) established in the South China Sea by Hong et al. (1997). The $\delta^{13}C$ at equilibrium is calculated based on the $\delta^{13}C$ value of the DIC at Sanya Bay (Deng et al., 2013), an aragonite-bicarbonate ^{13}C fractionation factor of 2.7‰ (Romanek et al., 1992), and an assumption that the DIC pool is dominated by bicarbonate ions.

of $\delta^{13}C$, $\delta^{18}O$, and Δ_{47} have previously been defined as the offsets of measured values relative to their respective equilibrium values (Kimball et al., 2016; Saenger et al., 2012; Spooner et al., 2016; Thiagarajan et al., 2011). In our study, we defined the Δ values as the offsets of the binned isotopic compositions in track 16SYST1 relative to 16SYST2 (Figures 5a and 5b). In addition to the comparison with Saenger et al.'s (2012) data, we also showed the offsets of measured values from the two tracks relative to their respective equilibrium values (Figures 5c and 5d). The processes of diffusion, hydration, and hydroxylation of metabolic CO_2 have been considered as important factors controlling the isotopic composition of corals (Saenger et al., 2012; Spooner et al., 2016). The corresponding $\Delta(\Delta_{47})/\Delta(\delta^{18}O)$ and $\Delta(\Delta_{47})/\Delta(\delta^{13}C)$ ratios are considered below.

(1) Metabolic CO_2 enters the coral calcifying sites via diffusion across the cell membrane. This can involve kinetic isotope fractionation (KIF), possibly resulting in depletion of $\delta^{13}C$ by 0.7‰ and $\delta^{18}O$ by 1.6‰, along with enrichment of Δ_{47} by 0.036‰ (Thiagarajan et al., 2011). The corresponding $\Delta(\Delta_{47})/\Delta(\delta^{18}O)$ ratio is −0.02, and the $\Delta(\Delta_{47})/\Delta(\delta^{13}C)$ ratios is −0.05.

(2) The CO_2 hydration and hydroxylation in the coral internal DIC pool with rapid coral calcification are also associated with KIF (McConnaughey, 1989b). These kinetic effects increase the relative proportion of ^{13}C–^{18}O bonds in HCO_3^- or CO_3^{2-} species, leading to negative ratios of $\Delta(\Delta_{47})/\Delta(\delta^{18}O)$ in carbonates of the order of −0.01 to −0.05 at 25 °C (Guo, Kim, et al., 2009). The ratios of $\Delta(\Delta_{47})/\Delta(\delta^{13}C)$ estimated from theoretical calculations are −0.015 for hydration and −0.007 for hydroxylation, as calculated by dividing $\Delta(\Delta_{47})/\Delta(\delta^{18}O)$ by $\Delta(\delta^{13}C)/\Delta(\delta^{18}O)$ (Guo et al., 2008; Saenger et al., 2012).

Plotting these ratios versus isotopic offsets in the $\Delta(\Delta_{47})$-$\Delta(\delta^{18}O)$ panel indicates that the direction of isotopic fractionation is different to those obtained by Saenger et al. (2012) based on *Porites* corals (Figure 5a). The direction is not characteristic of the $\Delta(\Delta_{47})/\Delta(\delta^{18}O)$ slopes predicted for diffusion, hydration, or hydroxylation of CO_2. In the $\Delta(\Delta_{47})$-$\Delta(\delta^{13}C)$ panel, however, the isotopic fractionation direction is generally parallel to the hydration and hydroxylation slopes (Figure 5b), which is broadly consistent with the results reported by Saenger et al. (2012). Despite the possibility of errors arising from the theoretical predictions, the difference in directions of Δ_{47} fractionation suggests that mechanisms behind the observed Δ_{47} vital effects are also different between the two studies. The magnitude of the relative disequilibrium in Δ_{47} values at intracolony level in this study is at times higher than 0.02‰, especially when growth temperatures are higher than 28 °C (Figures 5a and 5b). This magnitude is comparable to that observed by Saenger et al. (2012), and this study based on seawater equilibrium (Figures 5c and 5d). This suggests that Δ_{47} disequilibrium at the intracolony level on seasonal timescales is also significant and could compound the positive Δ_{47} offset observed in *Porites* corals relative to inorganic carbonate.

The origin of $\delta^{13}C$ and Δ_{47} differences observed in the two sampling tracks is possibly related to the growth rates of the coral skeletons, as high coral skeletal growth rate likely results in lower $\delta^{13}C$ and higher Δ_{47} values (McConnaughey, 1989a, 1989b; Omata et al., 2005; Saenger et al., 2012; Suzuki et al., 2005). However, growth rates on a seasonal timescale are difficult to measure precisely. Assuming a linear growth rate and an annual calcification rate in proportion to the seasonal growth rates enables us to compare the seasonal growth rates of the two sampling tracks. Following the relationship between calcification rate and linear extension rate established based on *Porites* coral colonies from 49 reefs (Lough, 2008; Saenger et al., 2012), we estimated the annual calcification rates of ~4.8 mg cm^{-2} d^{-1} for 16SYST1 and ~4.5 mg cm^{-2} d^{-1} for 16SYST2. However, the difference between the two calcification rates is too small to explain the difference in Δ_{47} values, particularly considering the results of Saenger et al. (2012), in which they observed Δ_{47} offsets from ~0.019‰ to 0.042‰ over a calcification rate range of 1.0–3.5 mg cm^{-2} d^{-1}. As such, differences in seasonal growth rates are probably not a major factor controlling the $\delta^{13}C$ and Δ_{47} differences at the intracolony level. Although the cause(s) of the relative disequilibrium of isotopic compositions remains unclear, the evidence regarding the influence of vital effects demonstrates the necessity of reconsidering the prediction of fractionation directions based on previous theoretical calculations (Guo, Kim, et al., 2009), which do not fully take into account the vital effects that affect Δ_{47} in biogenic carbonates.

It is also uncertain if the fractionation directions combined with two isotope systems are acceptable to capture or distinguish the main features of different fractionation processes (e.g., CO_2 diffusion or hydration). Recent studies have observed significant decoupling of the Δ_{47} and $\delta^{18}O$ in DIC during isotopic equilibrium (Guo et al., 2019; Staudigel & Swart, 2018). By numerical modeling and theoretical calculations, Guo (2020) also found the nonlinear behaviors of the Δ_{47} and $\delta^{18}O$ in DIC during the equilibrium and suggested that mixing or removal of DIC species that have undergone kinetic fractionation is likely the main control of the Δ_{47} disequilibrium observed in DIC and natural carbonates. These results imply that the vital effect on isotopic compositions may be a result of multiple processes instead of being dominated by a single mechanism. Nevertheless, further deciphering the cause(s) of the relative Δ_{47} disequilibrium at the intracolony level will be benefit from additional theoretical and experimental work.

4.2. Temperature Dependence of Coral Δ_{47}

With previous studies have shown that vital effects can influence the Δ_{47} values of *Porites* coral, they have also demonstrated a clear temperature dependence (Saenger et al., 2012). Further application of Δ_{47} as a paleotemperature proxy must consider any intercolony and intracolony differences that may affect this temperature dependence. On annual timescales, the effects of intercolony differences on the Δ_{47} values are

Table 2
T Test of the Mean Differences of Δ_{47} Values

Comparison	Mean difference (‰)	*T* test calculated value	*T* test critical value ($\alpha = 0.05$)
16SYS (T1 and T2) versus 15XS15	−0.005	1.54	2.00
16SYST1 versus 16SYST2	0.006	1.16	2.03

Note. For each comparison, the two groups of values are verified by a normality test, which indicates that at the 95% confidence level each data group are significantly drawn from a normally distributed population. *T* tests further verifies that at the 95% confidence level there is no statistically significant difference between mean values of the two groups.

insignificant, as the mean Δ_{47} values of colonies from Sanya Bay (16SYS) and Qilianyu Islet (15XS) are not significantly different (based on student's *t* test; Table 2). There was also no significant difference between the mean Δ_{47} values of the two sampling tracks from the Sanya Bay colony (16SYST1 and 16SYST2; Table 2). This suggests that intercolony and intracolony differences do not affect the annual Δ_{47} values in *Porites* corals.

To investigate the temperature dependence of coral Δ_{47} values on seasonal timescales, we compared the Δ_{47} values with growth temperatures for the three sampling tracks (Figures 6a–6c). The resulting Δ_{47}-T calibration curves of the three sampling tracks have positive slopes, which indicates thermodynamic control of the clumped isotopic composition as suggested by theoretical predications (Guo, Mosenfelder, et al., 2009; Schauble et al., 2006). The three sample tracks exhibit different slopes, although those of

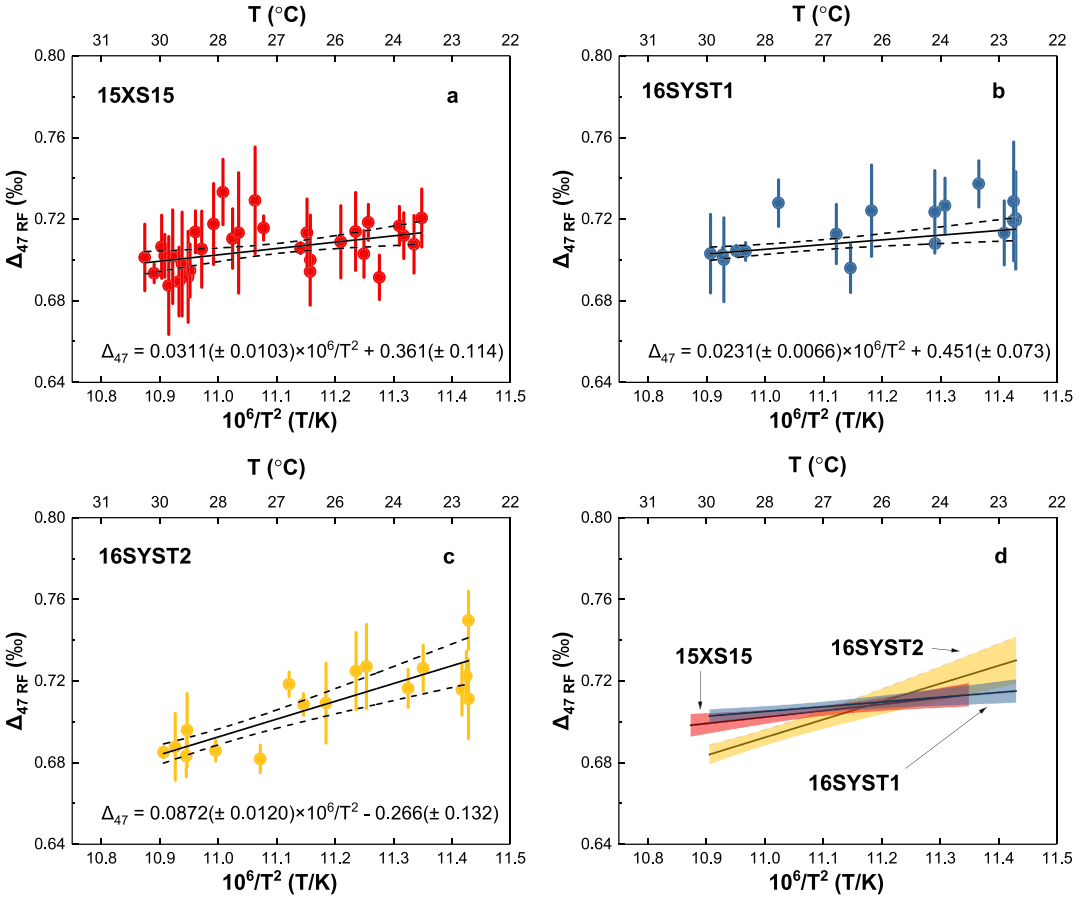

Figure 6. Temperature dependence of coral Δ_{47} values among the three sampling tracks. (a) 15XS15; (b) 16SYST1; (c) 16SYST2; (d) comparison of the three sampling tracks. The growth temperatures are estimated based on satellite-derived SST records. The dashed lines or shaded envelopes indicate 95% confidence intervals. The T/K indicates temperatures in kelvin units.

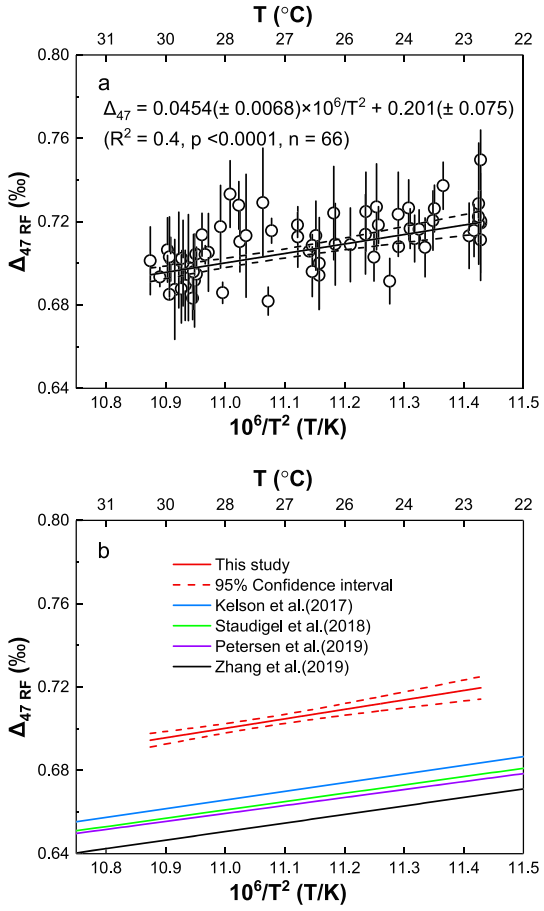

Figure 7. The coral Δ_{47}–T relationship derived from this study, compared with inorganic and synthetic calibrations. (a) Linear fitting based on all coral data; (b) comparison of linear fitting with recently published inorganic calibrations (Kelson et al., 2017; Staudigel et al., 2018) and synthetic calibrations (Petersen et al., 2019; Zhang et al., 2019). Note that all Δ_{47} values of the calibrations were adjusted with the same AFF value of 0.068‰ and processed with the ^{17}O correction method of Brand et al. (2010). The T/K indicates temperatures in kelvin units.

the 16SYST1 and 15XS15 are similar (Figure 6d). We do not consider that these differences are solely the result of intercolony or intracolony biases. The significant variation between these slopes is likely associated with the low number of sample points or the limited range of temperatures investigated, which has been noted to be important in calibration studies (Bonifacie et al., 2017; Fernandez et al., 2017; Kelson et al., 2017). Consequently, the differences in slopes and intercepts among the three tracks are not sufficiently large as to suggest an intercolony or intracolony bias but are more likely at least in part derived from analytical noise (or random error). To reduce such noise and take into account possible intercolony or intracolony variation, we combined all the data to form a single Δ_{47}-T calibration line (Figure 7a):

$$\Delta_{47} = 0.0454\ (\pm 0.0068) \times 10^6/T^2 + 0.201\ (\pm 0.075). \quad (2)$$

The three sampling tracks are derived from coral colonies that are from both inshore and offshore settings influenced by different environmental variables, including continental input, rainfall, tidal variations and local currents, and nutrient fluctuations. Therefore, this calibration provides a "universal" empirical line specific to *Porites* corals for SST reconstruction and will likely be applicable in various environmental conditions.

The single Δ_{47}-T calibration line derived here has a similar slope to several recently published calibrations based on different sources of carbonates (Kelson et al., 2017; Petersen et al., 2019; Staudigel et al., 2018; Zhang et al., 2019) with a intercept that is positively offset relative to those of the four previous calibrations (Figure 7b). This suggests that the Δ_{47} values of *Porites* corals share a similar temperature dependence to that indicated in inorganic calibrations while being also affected by vital effects. Note that the variation of the offset can be partly caused by using different values of AFF (ranging from 0.066‰ to 0.092‰ for calcite or aragonite) among the calibrations (Guo et al., 2019; Henkes et al., 2013; Wacker et al., 2013), leading to less precise evaluation of the magnitude of vital effects. To avoid such situation, we applied the same AFF of 0.068‰ for all the calibrations when comparing them with our calibration. It also should be noted that using a same AFF for all samples is potentially problematic because the AFF can be affected by the carbonate's initial Δ_{47} value, leading to less precise estimation of carbonate formation temperature (Swart et al., 2019). This situation likely results from ^{13}C–^{18}O bond reordering as a function of acid digestion temperature, which could be significant when comparing the AFFs of samples that have large difference (more than ~0.2‰) in their Δ_{47} values (Swart et al., 2019). However, considering the small variation of Δ_{47} values (less than ~0.07‰) of samples addressed in this study, we think that using the same AFF here is appropriate and has less effect on the our Δ_{47}-T calibration.

In this study, the mean Δ_{47} offset is ~0.04‰ relative to the calibration of Kelson et al. (2017). As observed by Saenger et al. (2012), this offset is not temperature dependent and is constant during coral's growth. This allows correction to be made accounting for the offset and enables determination of SST from coral Δ_{47}. However, SST reconstructions should be conducted with caution, as we have demonstrated the constancy of the Δ_{47} offset only within the temperature range of 22–30 °C. Furthermore, due to the offsets observed, we are only able to reconstruct relative changes in seasonal SST using this *Porites* calibration, rather than absolute temperature reconstructions. With further improvements in the sampling resolution or reducing the sample size typically required for clumped isotope measurements, the relative changes in monthly SST could be examined. In this regard, our study holds a promise for using clumped isotopes in fossil corals to study paleo-SST variations.

5. Conclusions

On annual timescales, intercolony and intracolony variations in Δ_{47} values are not significant. However, on seasonal timescales, we found a relative offset of more than 0.02‰ in Δ_{47} between two isochronal skeletons within the same colony. Such intracolony variation corresponds to a temperature uncertainty of ~6 °C at 25 °C and is related to coral vital effects with a unique pattern of isotopic fractionation that cannot be explained by the kinetic effects of the CO_2 hydration/hydroxylation process. However, despite vital effects and systematic Δ_{47} enrichments relative to inorganic carbonates, *Porites* coral Δ_{47} values still exhibit a similar temperature dependence to that of inorganic carbonates. This clear temperature dependence of Δ_{47} signatures in two modern *Porites* corals strengthens the potential of clumped isotopes for use in SST reconstructions. An empirical calibration was derived on the basis of coral Δ_{47} data, which can potentially be used to derive relative variations in seasonal SST. This study makes a valuable contribution to future paleoclimate studies using *Porites* corals.

Acknowledgments
The coral samples were collected under the permission of the Department of Ocean and Fisheries of Hainan Province. The ETH standards were provided by Dr. Stefano M. Bernasconi. We thank Dr. Miguel Goni and two anonymous reviewers for their valuable suggestion. This work was supported by the National Key Research and Development Program of China (2016YFA0601204), the Key Special Project for Introduced Talents Team of Southern Marine Science and Engineering Guangdong Laboratory (Guangzhou) (GML2019ZD0308), the National Natural Science Foundation of China (41722301, 41673115, and 41173004), the Project of China Geological Survey (DD20190627), the Guangzhou Institute of Geochemistry, Chinese Academy of Sciences (135PY201605), and the Technology Research and Development Project of the Chinese Academy of Sciences (yg2010021). This is contribution No. IS-2768 from GIGCAS. Raw isotopic data are available on Zenodo (https://doi.org/10.5281/zenodo.3525788). The authors declare no conflicts of interest from their funding or affiliations.

References

Beck, J. W., Edwards, R. L., Ito, E., Taylor, F. W., Recy, J., Rougerie, F., et al. (1992). Sea-surface temperature from coral skeletal strontium/calcium ratios. *Science*, *257*(5070), 644–647. https://doi.org/10.1126/science.257.5070.644

Bonifacie, M., Calmels, D., Eiler, J. M., Horita, J., Chaduteau, C., Vasconcelos, C., et al. (2017). Calibration of the dolomite clumped isotope thermometer from 25 to 350 °C, and implications for a universal calibration for all (Ca, Mg, Fe) CO_3 carbonates. *Geochimica et Cosmochimica Acta*, *200*, 255–279. https://doi.org/10.1016/j.gca.2016.11.028

Brand, W. A., Assonov, S. S., & Coplen, T. B. (2010). Correction for the ^{17}O interference in $\delta(^{13}C)$ measurements when analyzing CO_2 with stable isotope mass spectrometry (IUPAC Technical Report). *Pure and Applied Chemistry*, *82*(8), 1719–1733. https://doi.org/10.1351/pac-rep-09-01-05

Daëron, M., Blamart, D., Peral, M., & Affek, H. P. (2016). Absolute isotopic abundance ratios and the accuracy of Δ_{47} measurements. *Chemical Geology*, *442*, 83–96. https://doi.org/10.1016/j.chemgeo.2016.08.014

de Villiers, S., Nelson, B. K., & Chivas, A. R. (1995). Biological controls on coral Sr/Ca and $\delta^{18}O$ reconstructions of sea surface temperatures. *Science*, *269*(5228), 1247–1249. https://doi.org/10.1126/science.269.5228.1247

Deng, W., Wei, G., Xie, L., & Yu, K. (2013). Environmental controls on coral skeletal $\delta^{13}C$ in the northern South China Sea. *Journal of Geophysical Research: Biogeosciences*, *118*, 1359–1368. https://doi.org/10.1002/jgrg.20116

Dennis, K. J., Affek, H. P., Passey, B. H., Schrag, D. P., & Eiler, J. M. (2011). Defining an absolute reference frame for "clumped" isotope studies of CO_2. *Geochimica et Cosmochimica Acta*, *75*(22), 7117–7131. https://doi.org/10.1016/j.gca.2011.09.025

Eiler, J. M. (2007). "Clumped-isotope" geochemistry—The study of naturally-occurring, multiply-substituted isotopologues. *Earth and Planetary Science Letters*, *262*(3-4), 309–327. https://doi.org/10.1016/j.epsl.2007.08.020

Felis, T., Pätzold, J., & Loya, Y. (2003). Mean oxygen-isotope signatures in Porites spp. corals: Inter-colony variability and correction for extension-rate effects. *Coral Reefs*, *22*(4), 328–336. https://doi.org/10.1007/s00338-003-0324-3

Felis, T., Patzold, J., Loya, Y., Fine, M., Nawar, A. H., & Wefer, G. (2000). A coral oxygen isotope record from the northern Red Sea documenting NAO, ENSO, and North Pacific teleconnections on Middle East climate variability since the year 1750 (Paper 1999PA000477). *Paleoceanography*, *15*(6), 679–694.

Fernandez, A., Muller, I. A., Rodriguez-Sanz, L., van Dijk, J., Looser, N., & Bernasconi, S. M. (2017). A reassessment of the precision of carbonate clumped isotope measurements: Implications for calibrations and paleoclimate reconstructions. *Geochemistry, Geophysics, Geosystems*, *18*, 4375–4386. https://doi.org/10.1002/2017GC007106

Gagan, M. K., Ayliffe, L. K., Hopley, D., Cali, J. A., Mortimer, G. E., Chappell, J., et al. (1998). Temperature and surface-ocean water balance of the mid-Holocene tropical western Pacific. *Science*, *279*(5353), 1014–1018.

Ghosh, P., Adkins, J., Affek, H., Balta, B., Guo, W., Schauble, E. A., et al. (2006). ^{13}C–^{18}O bonds in carbonate minerals: A new kind of paleothermometer. *Geochimica et Cosmochimica Acta*, *70*(6), 1439–1456. https://doi.org/10.1016/j.gca.2005.11.014

Goreau, T. J. (1977). Coral skeletal chemistry: Physiological and environmental regulation of stable isotopes and trace metals in Montastrea annularis. *Proceedings of the Royal Society of London, Series B: Biological Sciences*, *196*(1124), 291–315. https://doi.org/10.1098/rspb.1977.0042

Guo, W. (2020). Kinetic clumped isotope fractionation in the DIC-H_2O-CO_2 system: Patterns, controls, and implications. *Geochimica et Cosmochimica Acta*, *268*, 230–257. https://doi.org/10.1016/j.gca.2019.07.055

Guo, W., Daeron, M., Niles, P., Genty, D., Kim, S.-T., Vonhof, H., et al. (2008). ^{13}C-^{18}O bonds in dissolved inorganic carbon: Implications for carbonate clumped isotope thermometry. *Geochimica et Cosmochimica Acta*, *72*(12), A336–A336.

Guo, W., Kim, S., Thiagarajan, N., Adkins, J., & Eiler, J. (2009). Mechanisms for "Vital Effects" in biogenic carbonates: New perspectives based on abundances of ^{13}C-^{18}O bonds, paper presented at AGU Fall Meeting Abstracts.

Guo, W., Mosenfelder, J. L., Goddard, W. A., & Eiler, J. M. (2009). Isotopic fractionations associated with phosphoric acid digestion of carbonate minerals: Insights from first-principles theoretical modeling and clumped isotope measurements. *Geochimica et Cosmochimica Acta*, *73*(24), 7203–7225. https://doi.org/10.1016/j.gca.2009.05.071

Guo, Y. (2019). Supplementary Dataset for "Exploring the temperature dependence of clumped isotopes in modern Porites corals". https://doi.org/10.5281/zenodo.3525788.

Guo, Y. R., Deng, W. F., & Wei, G. J. (2019). Kinetic effects during the experimental transition of aragonite to calcite in aqueous solution: Insights from clumped and oxygen isotope signatures. *Geochimica et Cosmochimica Acta*, *248*, 210–230. https://doi.org/10.1016/j.gca.2019.01.012

Hammer, Ř., Harper, D., & Ryan, P. (2001). PAST: Paleontological statistics software package for education and data analysis. *Palaeontologia Electronica*, *4*, 1–9.

Henkes, G. A., Passey, B. H., Wanamaker, A. D., Grossman, E. L., Ambrose, W. G., & Carroll, M. L. (2013). Carbonate clumped isotope compositions of modern marine mollusk and brachiopod shells. *Geochimica et Cosmochimica Acta*, *106*, 307–325. https://doi.org/10.1016/j.gca.2012.12.020

Hong, A., Hong, Y., Wang, Q., Ke, J., Huang, Y., & Liu, Y. (1997). Distributive characteristics of O isotope of the northeastern South China Sea in the summer of 1994 [in Chinese]. *Tropic Oceanology*, *16*(2), 82–90.

Huntington, K. W., Eiler, J. M., Affek, H. P., Guo, W., Bonifacie, M., Yeung, L. Y., et al. (2009). Methods and limitations of "clumped" CO_2 isotope (Δ_{47}) analysis by gas-source isotope ratio mass spectrometry. *Journal of Mass Spectrometry: JMS*, *44*(9), 1318–1329. https://doi.org/10.1002/jms.1614

John, C. M., & Bowen, D. (2016). Community software for challenging isotope analysis: First applications of "Easotope" to clumped isotopes. *Rapid Communications in Mass Spectrometry*, *30*(21), 2285–2300.

Kelson, J. R., Huntington, K. W., Schauer, A. J., Saenger, C., & Lechler, A. R. (2017). Toward a universal carbonate clumped isotope calibration: Diverse synthesis and preparatory methods suggest a single temperature relationship. *Geochimica et Cosmochimica Acta*, *197*, 104–131. https://doi.org/10.1016/j.gca.2016.10.010

Kim, S.-T., Mucci, A., & Taylor, B. E. (2007). Phosphoric acid fractionation factors for calcite and aragonite between 25 and 75 °C: Revisited. *Chemical Geology*, *246*(3-4), 135–146. https://doi.org/10.1016/j.chemgeo.2007.08.005

Kim, S.-T., O'Neil, J. R., Hillaire-Marcel, C., & Mucci, A. (2007). Oxygen isotope fractionation between synthetic aragonite and water: Influence of temperature and Mg^{2+} concentration. *Geochimica et Cosmochimica Acta*, *71*(19), 4704–4715. https://doi.org/10.1016/j.gca.2007.04.019

Kimball, J., Tripati, R., & Dunbar, R. (2016). Carbonate "clumped" isotope signatures in aragonitic scleractinian and calcitic gorgonian deep-sea corals. *Biogeosciences*, *13*(23), 6487–6505.

Linsley, B. K., Messier, R. G., & Dunbar, R. B. (1999). Assessing between-colony oxygen isotope variability in the coral Porites lobata at Clipperton Atoll. *Coral Reefs*, *18*(1), 13–27. https://doi.org/10.1007/s003380050148

Lough, J. M. (2008). Coral calcification from skeletal records revisited. *Marine Ecology Progress Series*, *373*, 257–264. https://doi.org/10.3354/meps07398

McConnaughey, T. (1989a). ^{13}C and ^{18}O isotopic disequilibrium in biological carbonates: I. Patterns. *Geochimica et Cosmochimica Acta*, *53*(1), 151–162. https://doi.org/10.1016/0016-7037(89)90282-2

McConnaughey, T. (1989b). ^{13}C and ^{18}O isotopic disequilibrium in biological carbonates: II. *In vitro* simulation of kinetic isotope effects. *Geochimica et Cosmochimica Acta*, *53*(1), 163–171. https://doi.org/10.1016/0016-7037(89)90283-4

McCulloch, M. T., Tudhope, A. W., Esat, T. M., Mortimer, G. E., Chappell, J., Pillans, B., et al. (1999). Coral record of equatorial sea-surface temperatures during the penultimate deglaciation at Huon Peninsula. *Science*, *283*(5399), 202–204. https://doi.org/10.1126/science.283.5399.202

Merritt, D. A., & Hayes, J. M. (1994). Factors controlling precision and accuracy in isotope-ratio-monitoring mass spectrometry. *Analytical Chemistry*, *66*(14), 2336–2347. https://doi.org/10.1021/ac00086a020

Mitsuguchi, T., Matsumoto, E., & Uchida, T. (2003). Mg/Ca and Sr/Ca ratios of Porites coral skeleton: Evaluation of the effect of skeletal growth rate. *Coral Reefs*, *22*(4), 381–388. https://doi.org/10.1007/s00338-003-0326-1

Omata, T., Suzuki, A., Kawahat, H., & Okamoto, M. (2005). Annual fluctuation in the stable carbon isotope ratio of coral skeletons: The relative intensities of kinetic and metabolic isotope effects. *Geochimica et Cosmochimica Acta*, *69*(12), 3007–3016.

Petersen, S. V., Defliese, W. F., Saenger, C., Daëron, M., Huntington, K. W., John, C. M., et al. (2019). Effects of improved ^{17}O correction on interlaboratory agreement in clumped isotope calibrations, estimates of mineral-specific offsets, and temperature dependence of acid digestion fractionation. *Geochemistry, Geophysics, Geosystems*, *20*, 3495–3519. https://doi.org/10.1029/2018GC008127

Romanek, C. S., Grossman, E. L., & Morse, J. W. (1992). Carbon isotopic fractionation in synthetic aragonite and calcite: Effects of temperature and precipitation rate. *Geochimica et Cosmochimica Acta*, *56*(1), 419–430. https://doi.org/10.1016/0016-7037(92)90142-6

Saenger, C., Affek, H. P., Felis, T., Thiagarajan, N., Lough, J. M., & Holcomb, M. (2012). Carbonate clumped isotope variability in shallow water corals: Temperature dependence and growth-related vital effects. *Geochimica et Cosmochimica Acta*, *99*, 224–242. https://doi.org/10.1016/j.gca.2012.09.035

Saenger, C., Gabitov, R. I., Farmer, J., Watkins, J. M., & Stone, R. (2017). Linear correlations in bamboo coral $\delta^{13}C$ and $\delta^{18}O$ sampled by SIMS and micromill: Evaluating paleoceanographic potential and biomineralization mechanisms using $\delta^{11}B$ and Δ_{47} composition. *Chemical Geology*, *454*, 1–14. https://doi.org/10.1016/j.chemgeo.2017.02.014

Schauble, E. A., Ghosh, P., & Eiler, J. M. (2006). Preferential formation of ^{13}C–^{18}O bonds in carbonate minerals, estimated using first-principles lattice dynamics. *Geochimica et Cosmochimica Acta*, *70*(10), 2510–2529. https://doi.org/10.1016/j.gca.2006.02.011

Schauer, A. J., Kelson, J., Saenger, C., & Huntington, K. W. (2016). Choice of ^{17}O correction affects clumped isotope Δ_{47} values of CO_2 measured with mass spectrometry. *Rapid Communications in Mass Spectrometry*, *30*(24), 2607–2616. https://doi.org/10.1002/rcm.7743

Schoepf, V., Levas, S. J., Rodrigues, L. J., McBride, M. O., Aschaffenburg, M. D., Matsui, Y., et al. (2014). Kinetic and metabolic isotope effects in coral skeletal carbon isotopes: A re-evaluation using experimental coral bleaching as a case study. *Geochimica et Cosmochimica Acta*, *146*, 164–178. https://doi.org/10.1016/j.gca.2014.09.033

Shackleton, N. J. (1967). Oxygen isotope analyses and Pleistocene temperatures re-assessed. *Nature*, *215*(5096), 15–17.

Smith, S., Buddemeier, R., Redalje, R., & Houck, J. (1979). Strontium-calcium thermometry in coral skeletons. *Science*, *204*(4391), 404–407. https://doi.org/10.1126/science.204.4391.404

Spooner, P. T., Guo, W., Robinson, L. F., Thiagarajan, N., Hendry, K. R., Rosenheim, B. E., & Leng, M. J. (2016). Clumped isotope composition of cold-water corals: A role for vital effects? *Geochimica et Cosmochimica Acta*, *179*, 123–141. https://doi.org/10.1016/j.gca.2016.01.023

Staudigel, P. T., Murray, S., Dunham, D. P., Frank, T. D., Fielding, C. R., & Swart, P. K. (2018). Cryogenic brines as diagenetic fluids: Reconstructing the diagenetic history of the Victoria Land Basin using clumped isotopes. *Geochimica et Cosmochimica Acta*, *224*, 154–170. https://doi.org/10.1016/j.gca.2018.01.002

Staudigel, P. T., & Swart, P. K. (2016). Isotopic behavior during the aragonite-calcite transition: Implications for sample preparation and proxy interpretation. *Chemical Geology*, *442*, 130–138. https://doi.org/10.1016/j.chemgeo.2016.09.013

Staudigel, P. T., & Swart, P. K. (2018). A kinetic difference between ^{12}C- and ^{13}C-bound oxygen exchange rates results in decoupled $\delta^{18}O$ and Δ_{47} values of equilibrating DIC solutions. *Geochemistry, Geophysics, Geosystems*, *19*, 2371–2383. https://doi.org/10.1029/2018GC007500

Suzuki, A., Hibino, K., Iwase, A., & Kawahata, H. (2005). Intercolony variability of skeletal oxygen and carbon isotope signatures of cultured *Porites* corals: Temperature-controlled experiments. *Geochimica et Cosmochimica Acta*, *69*(18), 4453–4462.

Swart, P. K., Murray, S. T., Staudigel, P. T., & Hodell, D. A. (2019). Oxygen isotopic exchange between CO_2 and phosphoric acid: Implications for the measurement of clumped isotopes in carbonates. *Geochemistry, Geophysics, Geosystems*, *20*, 3730–3750. https://doi.org/10.1029/2019GC008209

Thiagarajan, N., Adkins, J., & Eiler, J. (2011). Carbonate clumped isotope thermometry of deep-sea corals and implications for vital effects. *Geochimica et Cosmochimica Acta*, *75*(16), 4416–4425. https://doi.org/10.1016/j.gca.2011.05.004

Wacker, U., Fiebig, J., & Schoene, B. R. (2013). Clumped isotope analysis of carbonates: Comparison of two different acid digestion techniques. *Rapid Communications in Mass Spectrometry*, *27*(14), 1631–1642. https://doi.org/10.1002/rcm.6609

Wang, X., Deng, W., Liu, X., Wei, G., Chen, X., Zhao, J.-x., et al. (2018). Super instrumental El Niño events recorded by a Porites coral from the South China Sea. *Coral Reefs*, *37*(1), 295–308.

Wang, Z. G., Schauble, E. A., & Eiler, J. M. (2004). Equilibrium thermodynamics of multiply substituted isotopologues of molecular gases. *Geochimica et Cosmochimica Acta*, *68*(23), 4779–4797. https://doi.org/10.1016/j.gca.2004.05.039

Weber, J. N. (1974). Basis for skeletal plasticity among reef-building corals. *Geology*, *2*(3), 153–154.

Weber, J. N., & Woodhead, P. M. (1972). Temperature dependence of oxygen-18 concentration in reef coral carbonates. *Journal of Geophysical Research*, *77*(3), 463–473.

Wei, G. J., Deng, W. F., Yu, K. F., Li, X. H., Sun, W. D., & Zhao, J. X. (2007). Sea surface temperature records in the northern South China Sea from mid-Holocene coral Sr/Ca ratios. *Paleoceanography*, *22*, PA3206. https://doi.org/10.1029/2006PA001270

Zhang, N. Z., Lin, M., Snyder, G. T., Kakizaki, Y., Yamada, K., Yoshida, N., & Matsumoto, R. (2019). Clumped isotope signatures of methane-derived authigenic carbonate presenting equilibrium values of their formation temperatures. *Earth and Planetary Science Letters*, *512*, 207–213. https://doi.org/10.1016/j.epsl.2019.02.005